

# DiffGLE: Differentiable Coarse-Grained Dynamics using Generalized Langevin Equation

Jinu Jeong<sup>1,3</sup>, Ishan Nadkarni<sup>2,3</sup> and Narayana. R. Aluru<sup>2,3\*</sup>

1. Department of Mechanical Science and Engineering, University of Illinois at Urbana–Champaign, Urbana, Illinois, 61801, United States
2. Walker Department of Mechanical Engineering, The University of Texas at Austin, Austin 78712, Texas, United States
3. Oden Institute for Computational Engineering and Sciences, The University of Texas at Austin, Austin 78712, Texas, United States

\* Correspondence to [aluru@utexas.edu](mailto:aluru@utexas.edu) (N.A.)

**Abstract:** Capturing the correct dynamics at the Coarse-Grained (CG) scale remains a central challenge in the advancement of systematic CG models for soft matter simulations. The Generalized Langevin Equation (GLE), rooted in the Mori-Zwanzig formalism, provides a robust framework for incorporating friction and stochastic forces into CG models, that are lost due to the reduction in degrees of freedom. Leveraging recent advancements in Automatic Differentiation (AD) and reformulating the non-Markovian GLE using a colored noise ansatz, we present a top-down approach for accurately parameterizing the non-Markovian GLE for different coarse-grained fluids that accurately reproduces the velocity-autocorrelation function of the original All-Atom (AA) model. We demonstrate our approach on two different fluids namely, SPC/E water and carbon dioxide which have distinct structure and dynamical characteristics. Importantly, by being end-to-end differentiable, this approach offers a simplified and efficient solution to achieving accurate CG dynamics, effectively bypassing the complexities inherent in most bottom-up methods.

## 1. Introduction

Coarse-grained (CG) models have become indispensable in molecular modeling, bridging the gap between high-resolution atomistic simulations and the study of systems at realistic length and timescales—levels of detail often unattainable through experimental methods. By mapping the high-resolution All-Atom (AA) model into a low-resolution CG representation, one seeks to reduce complexity while also preserving the important characteristics of the AA system. CG force-field development and parameterization has therefore been an important topic of research<sup>1</sup>. Many important thermodynamic properties can be derived as conditional averages from the atomistic system and accurately captured by what is called the many-body potential of mean force (MB-PMF). Numerous methods<sup>2-4</sup> based on the MB-PMF, among others, have demonstrated success in capturing both important structural and thermodynamic properties of diverse systems, including polymers, proteins, nanofluids, and more<sup>5-7</sup>.

Despite these notable advancements, molecular dynamics (MD) simulations using CG models often produce significantly erroneous predictions of the dynamic properties of the systems under investigation. Most notably it leads to faster dynamics compared to the AA system<sup>8-10</sup>. This can be advantageous in certain situations, such as achieving rapid equilibration, but in most cases, this severely restricts the use of these models for studying dynamic effects and transport properties at relevant timescales. This inaccuracy is typically attributed to two key factors. First, the reduction in friction caused by the "projected dynamics" of the degrees of freedom that have been eliminated, as described by Mori and Zwanzig<sup>11-13</sup>. Second, an inaccurate representation of the high-dimensional MB-PMF, which results in shifts in the relative energy barriers within the Free-Energy Landscape, thereby altering the

timescales of barrier crossing events<sup>14,15</sup>. Several recent works have tried to address this challenge and develop dynamically accurate CG models. For a detailed review of these methods we direct the readers to important reviews in Ref<sup>16-18</sup>. In theory the Mori-Zwanzig (MZ) formalism provides an exact approach to modeling the time evolution of the CG degrees of freedom, resulting in an equation of motion for the CG degrees of freedom, popularly known as the Generalized Langevin Equation (GLE). However, parameterizing the GLE is a daunting task due to the presence of frictional and stochastic forces which depend on the complex projected dynamics<sup>13</sup>, as given by the MZ formalism. These forces implicitly account for the effects of the degrees of freedom that have been averaged out when constructing the CG model and are related by the Fluctuation-Dissipation Theorem (FDT). To overcome this complexity, several approximations<sup>19-21</sup> have been proposed to simplify different terms within the GLE. These simplifications have facilitated the widespread application of the GLE in CG systems, giving rise to popular methods like Dissipative Particle Dynamics (DPD)<sup>22</sup>.

A further complexity arising from the projection operations in the MZ formalism is the time-dependence of the resulting forces, which leads to GLE which is non-Markovian. In this case, the friction and random forces depend on the entire history of the system's time evolution. Often, a Markovian assumption is made to simplify the problem, assuming a time-independent friction kernel that results in a uniform friction coefficient and Gaussian white noise. This assumption holds when there is a clear separation of timescales between the CG degrees of freedom and those that are removed from the AA system, where the random force fluctuations occur much faster than the CG bead motion. However, in many critical systems, this timescale separation is absent, causing the Markovian approximation to fail, and necessitating the use of a non-Markovian GLE<sup>23,24</sup>. Consequently, several studies have investigated memory effects in CG models, highlighting the importance of time dependence of the memory kernel<sup>17,25</sup> in not only improving the dynamic accuracy but also in capturing important physical effects of the

atomistic system<sup>26</sup>. These bottom-up approaches have demonstrated the capacity to systematically parameterize the friction kernel using rigorous principles of statistical mechanics<sup>17,25,27,28</sup>. However, approximations are often involved, like the “Q-approximation”, where the projected dynamics is approximated as the true dynamics to obtain friction forces from the Force-Autocorrelation Function obtained from atomistic data. While various other methods<sup>13,16,29</sup> have been proposed to overcome these challenges, they often require complex derivations of memory kernels, coupled with the intricate and resource-intensive nature of implementing the CG model. A simpler approach involves following a top-down approach of selecting a functional form for the friction kernel and then adjusting the parameters to match kinetic properties of the CG model, such as the Velocity Autocorrelation Function (VACF) of the CG sites. Classically, such optimization has been challenging and approximate methods have been used which compromise accuracy<sup>30</sup>.

However, recent advancements in machine learning have given rise to sophisticated optimization methods that allow for precise control of target quantities, even when they depend on several model parameters in a complex manner. Automatic Differentiation (AD)<sup>31–33</sup> is one such powerful technique that calculates gradients by systematically applying the chain rule to fundamental computational operations. This allows one to create an end-to-end Differentiable Simulator<sup>34–36</sup> where gradients of output quantities can be directly propagated through the entire simulation trajectory to optimize model parameters<sup>37–39</sup>. By leveraging AD capabilities and adjoint-state method, we show for the first time that the friction and random force terms in the non-Markovian GLE could be accurately parameterized in a top-down manner to match local dynamic properties like VACF for complex fluids like SPC/E water and carbon dioxide. This approach lets us bypass the complexities inherent in the "bottom-up" techniques discussed earlier, offering a simpler and efficient alternative.

The remainder of the paper is structured as follows: We begin by presenting the reformulation of non-Markovian GLE parameterization as a “filter learning” problem, followed by construction of the end-to-end differentiable simulator using the adjoint-state method. Finally, we showcase the results for the adjoint-state optimization and the corresponding predictions for different bulk fluids, namely SPC/E water, carbon dioxide, and also confined SPC/E water.

## 2. Method

The Mori-Zwanzig projection operator theory offers an exact framework for the time evolution of CG degrees of freedom by modelling only the most significant variables while systematically "projecting out" the irrelevant ones. This projection introduces frictional and random forces, which implicitly account for the excluded degrees of freedom, ultimately resulting in the CG equations of motion commonly known as the Generalized Langevin Equation:-

$$ma(t) = F_C(r) - \int_0^t \Gamma(t - \tau)v(\tau)d\tau + R(t) \quad (1)$$

where,  $m$ ,  $a(t)$ ,  $F_C(r)$ ,  $\Gamma(\tau)$ ,  $v(t - \tau)$ , and  $R(t)$  represent mass, acceleration, conservative force, memory kernel, velocity, and random force, respectively. The conservative force describes the contribution from the MB-PMF, which in our case is described as a pairwise additive potential obtained using the Relative Entropy Minimization<sup>4,40,41</sup>. In contrast, the non-conservative interactions account for memory effects and random forces that are not explicitly included in the CG coordinates. Friction and random forces satisfy the so-called FDT which is given as,

$$\langle R(t + \tau), R(t) \rangle = k_B T \Gamma(\tau) \quad (2)$$

where,  $\langle \cdot, \cdot \rangle$ ,  $k_B$ , and  $T$  are ensemble average, Boltzmann constant, and temperature, respectively. The left-hand side being the Random force Autocorrelation Function (RACF). Since the memory kernel is time-dependent, the FDT implies that the random forces are also time-correlated, resulting in a colored noise. Using a top-down strategy we now aim to predict the memory kernel that yields an accurate representation of local dynamical properties, such as the VACF, reframing the task as an inverse problem. We start by reformulating GLE by modeling the random force with colored noise ansatz.

$$R(t) = h * \mathcal{N}(0,1) \quad (3)$$

where  $h$  and  $\mathcal{N}(0,1)$  are convolution filter and standard normal distribution, respectively. We provide justification on the colored noise consistency in Supporting Information S1 and S2. Substituting this into FDT, the memory kernel can be simplified as below.

$$\Gamma(\tau) = \frac{\langle h, h \rangle}{k_B T} \quad (4)$$

The GLE can be rewritten below, which simply requires parameterization of the convolution filter without any constraint, automatically satisfying the FDT.

$$m\dot{a}(t) = F_C(r) - \int k_B T \langle h, h \rangle v(t - \tau) d\tau + h * \mathcal{N}(0,1) \quad (5)$$

Equation (5) provides the equations of motion for the CG coordinates in terms of the filter coefficients  $h$ . Once these filter coefficients are determined, a CG molecular dynamics simulation can be performed using Equation (5) to compute properties such as the Radial Distribution Function (RDF) and VACF. Alternatively, in the context of an inverse problem, one can fix the target quantity as the VACF obtained from the atomistic system and iteratively adjust the filter coefficients to match this target accurately. One possible way is to define a scalar loss between the target AA dynamical quantity and the CG dynamical quantity and

compute the gradients of this loss function with respect to the filter coefficient  $h$ . We call this the “filter learning” approach. Computing the gradient is however not straightforward, since one needs to essentially backpropagate through the whole MD trajectory. Such a direct differentiation suffers from two computational issues, mainly 1) the exploding gradient problem and 2) memory issues due to the cost of reverse-mode AD that scales linearly with the number of MD steps. Fortunately, recent advancements in adjoint-state based methods have been shown to deal with these issues by being extremely memory-efficient and robust<sup>39,42–44</sup>. As we discuss next, the adjoint-state method essentially uses constrained optimization and constructs an adjoint state, which is then used to compute the gradient by solving an augmented system in the forward and reverse direction in a memory efficient manner.

The overall procedure of our differentiable simulation is illustrated in Figure 1 (A). Starting from the initial conditions, the simulator evolves the system, governed by Equation (5), in time using the Velocity-Verlet integration algorithm. The trajectories are then used to calculate ensemble average time-correlation functions such as the VACF,  $C_{vv}(t) = \langle v(0) \cdot v(t) \rangle$ . We then define a Mean Squared Error (MSE) loss function  $\mathcal{L}$  between the CG VACF,  $C_{vv}^{CG}(t)$  and the ground truth AA VACF  $C_{vv}^{AA}(t)$ ,

$$\mathcal{L} = \frac{1}{T} \int_0^T (C_{vv}^{CG}(t) - C_{vv}^{AA}(t))^2 dt \quad (6)$$

where  $T$  is time duration of the simulation. Then utilizing the adjoint-state method allows us to compute the gradients of  $\mathcal{L}$  with respect to the learnable filter coefficients  $h$ . We now describe the key ideas central to the adjoint-state method.

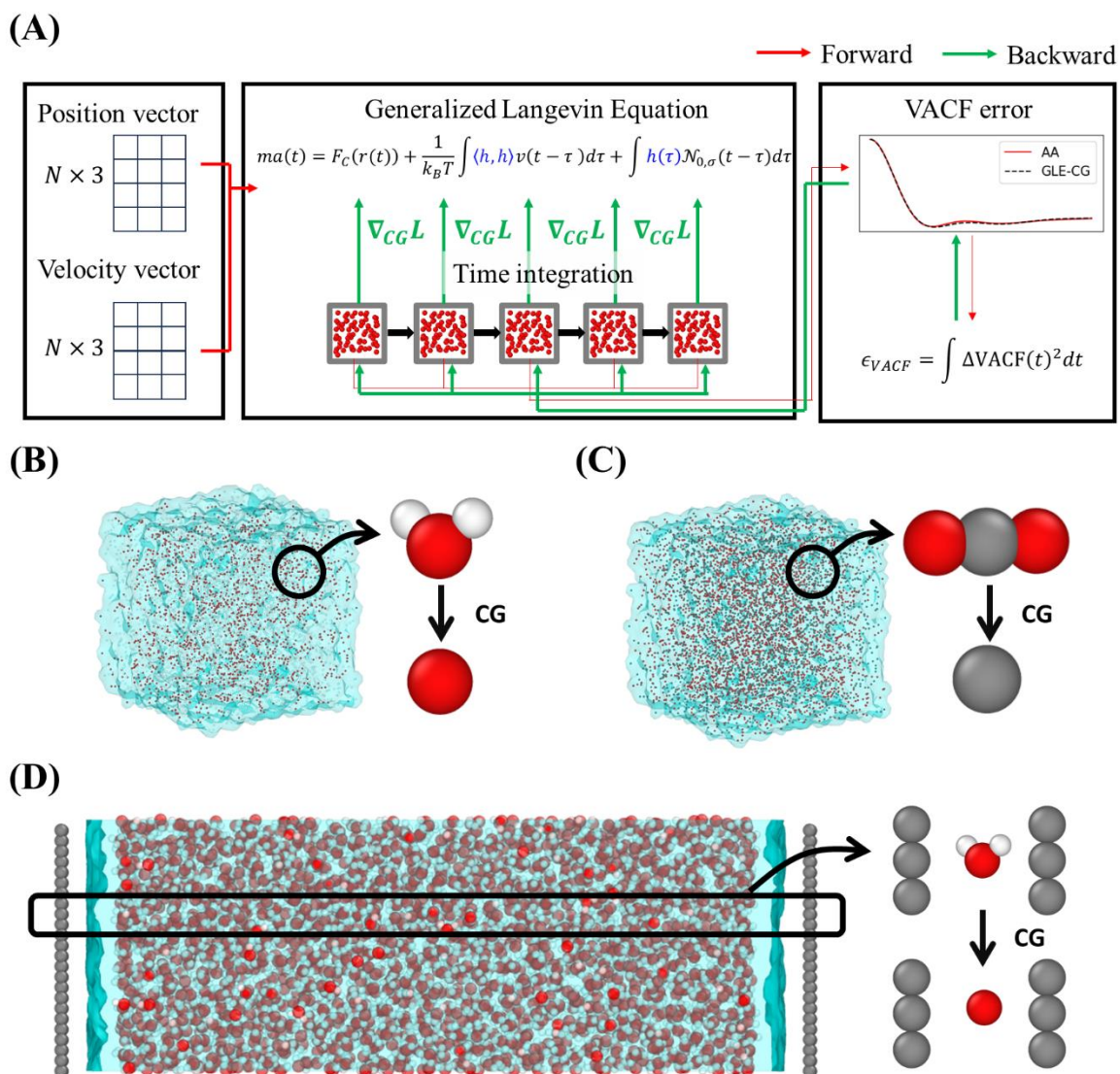


**Figure 1.** (A) Overview of the differentiable CGMD simulation framework integrating the optimization process. The simulator starts with initial conditions, uses the Velocity-Verlet algorithm for time integration, and employs post-processors to compute properties of interest, compare them with AA data, and calculate the loss function. Gradients of the loss function are computed using the adjoint-state method and used to update CG force field parameters via the ADAM optimizer. Different systems used – (B) Bulk SPC/E Water, (C) CO<sub>2</sub> and (D) confined SPC/E Water.



The time-evolution of the phase-space can be expressed using an ordinary differential equation, as below.

$$\frac{dr(t)}{dt} = f(r(t), t, h) \quad (7)$$

where  $t$ ,  $r(t)$ ,  $f$ , and  $h$  are time, atom positions at time  $t$ , function  $f$  (which depends on the time integrator) and filter coefficients  $h$ , respectively. The adjoint variable is then defined as the sensitivity of the loss function with respect to each trajectory.

$$a(t) = \frac{\partial \mathcal{L}}{\partial r(t)} \quad (8)$$

where  $a(t)$  is the adjoint variable at  $t$ . Applying the chain rule, this can be further evolved as below.

$$\frac{da(t)}{dt} = -a(t)^T \frac{\partial f(r(t), t, h)}{\partial r} \quad (9)$$

This is another differential equation, where its final condition ( $a(T)$ ) can be trivially calculated with AD, indicating that it is beneficial to solve the adjoint equation in time-reversal direction.

The gradient with respect to  $\theta$  can then be obtained by solving the following equation.

$$\frac{dL}{dh} = - \int_T^0 a(t)^T \frac{\partial f(r(t), t, h)}{\partial h} dt \quad (10)$$

We note that the adjoint-state method has been well-established for studying a variety of dynamical systems, including the application to molecular dynamics<sup>45</sup>, and we recommend referring to Ref <sup>39</sup> for more details of this method.

In practice, we iteratively perform and compute gradient in a piecewise manner, breaking the whole simulation trajectory into short-time durations of 1000 fs each, which is analogous to stochastic gradient descent, where working with smaller data segments allows for

more frequent updates to the parameters. Another point to note is that in NVE simulations, the backward trajectory can be retraced by solving the time-reversed equations of motion. However, in NVT simulations that incorporate GLE, this approach becomes problematic due to the presence of stochastic forces, which disrupt time reversibility. To resolve this, we store the state history for 1000 fs and the sampled noise in memory and utilize it during the simulation. While this approach increases memory usage linearly with time, it remains significantly more efficient than methods that do not employ the adjoint method. Once the gradient is computed, we update the CG force field parameters via the ADAM optimizer with an initial learning rate of  $3 \times 10^{-4}$ , which decays to  $1 \times 10^{-4}$  and  $1 \times 10^{-5}$  at 100 and 200 epoch of training. Additionally, we add a weight decay of  $1 \times 10^{-6}$  to regularize the parameter updates and prevent overfitting.

### 3. Result

The goal of the optimization is to refine the filter parameters by backpropagating the gradients described by Equation (10) starting from an initial guess of the filter coefficient. To test the robustness of the optimization scheme we try different initializations using various mathematical functions as shown in Table 1.

**Table 1.** Initial filter representations used in the optimization process.

Initial filter type	
Exponential 1	$e^{-0.01t}/200$
Exponential 2	$e^{-0.01t}/400$
Sine	$\sin(0.01t)/200$
Cosine	$\cos(0.01t)/400$

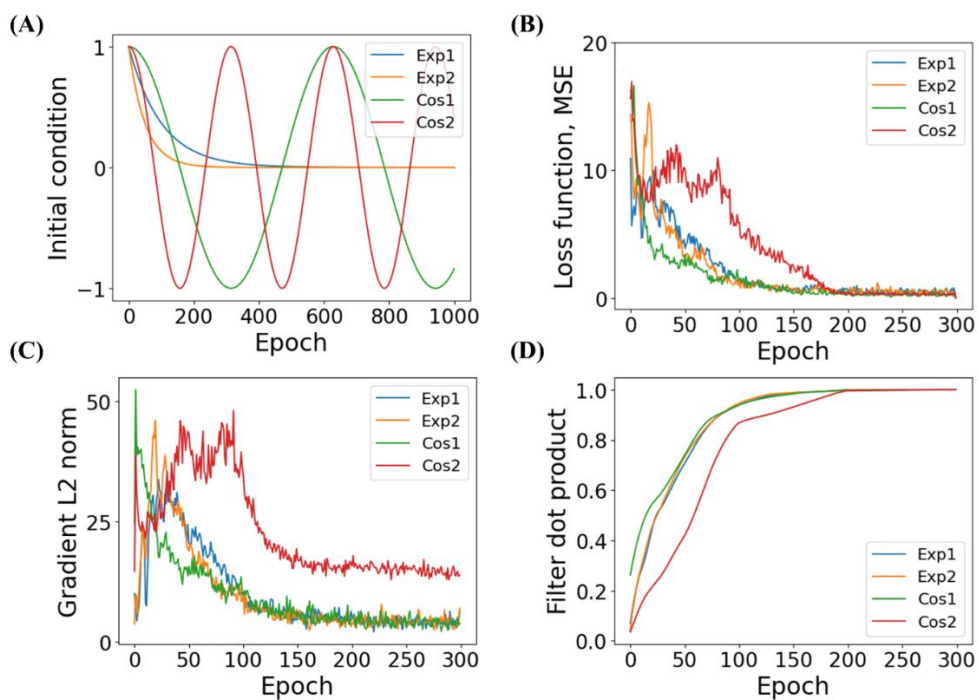


**Figure 2.** Performance of the optimization scheme for bulk water using different filter initialization strategies. (A) Different initializations of filter coefficients. (B) The MSE loss function plotted over 300 epochs, showing convergence for different initialization methods. (C) The L2 norm of the gradient of the loss function (D) The filter dot product with the converged filter across epochs.

The exponential function as an initial filter seems like a natural choice to simulate the gradual decay of the memory with time as is seen for most liquids. On the other hand, the sine and cosine functions were chosen to introduce a repeating pattern of decay and growth in their self-correlation, and to see if such oscillations create instabilities or convergence issues in the optimization process. We test different filter initializations for bulk SPC/E water, where the normalized filters are plotted on Figure 2 (A). Figure 2 (B) illustrates the decaying MSE loss function as the filter parameters are optimized. The gradient of MSE loss function is computed via the adjoint-state method. The L2 norm of gradient is visualized in Figure 2 (C), reflecting the rate of convergence. Figure 2 (D) presents the normalized dot product between the current filter and the optimal filter, indicating how close the intermediate filters were to the converged

solution. Both the metrics are seen to gradually converge to an optimal value. We initially used an exponential function as the filter for bulk water and carbon dioxide. Drawing an analogy to transfer learning, we then employed the filter optimized for bulk water as the initial filter for confined water. We applied our framework to three target systems: bulk SPC/E water, bulk carbon dioxide, and confined SPC/E water, as shown in Figure 1 (B-D). Detailed information about the system configuration and simulation settings is given in Supporting Information S3. We compute CG RDF and CG VACF and compare them with the corresponding AA ones. As shown in Figures 3 (A-C) and 3 (D-F), they are accurately reproduced. This indicates our CG model can reproduce both important structural and transport properties, therefore being dynamically accurate.

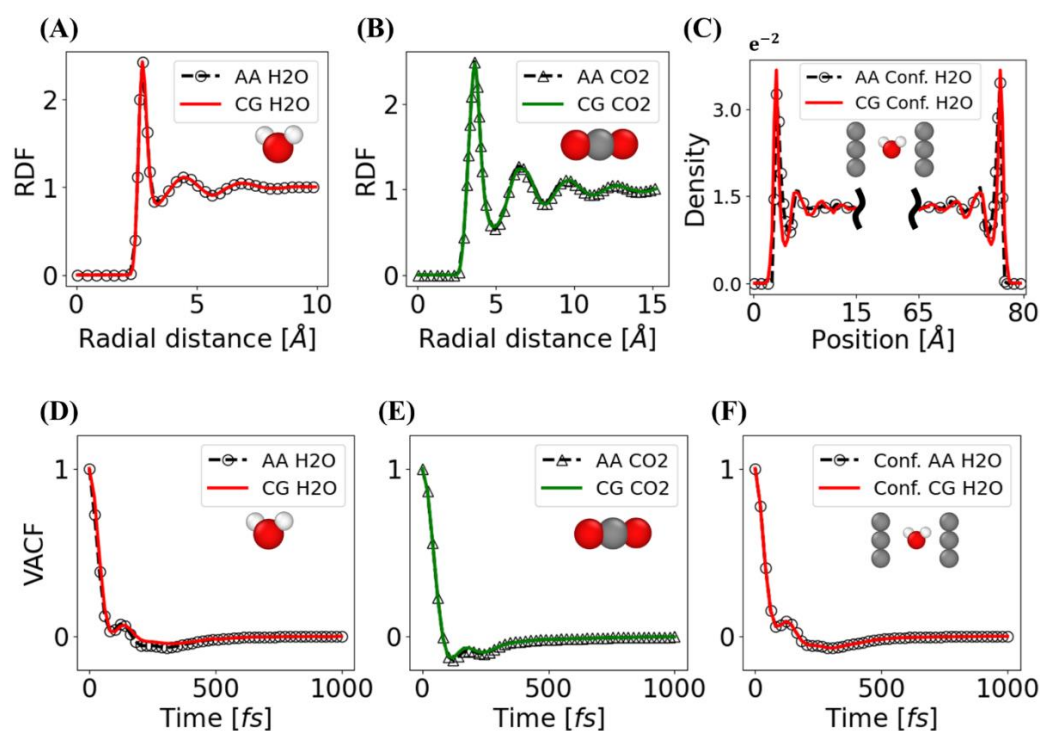


**Figure 3.** Comparison of the RDF and VACF between the CG model and the AA model. Bulk water, Bulk carbon dioxide, and confined water RDFs are shown in (A-C). VACFs for those molecules are shown in (D-F). The results demonstrate that the CG model accurately reproduces the RDF and VACF of the AA model, validating the effectiveness of the CGMD simulation framework.

We further show the convolution filter and memory kernel for the target systems that were learned from the differentiable simulations and are presented in Figures 4 (A-C) and 4 (D-F). Finally, we calculated the RACF from the random forces used in the simulations of each system and normalized them to compare with the normalized memory kernel to demonstrate that the generated colored noise and friction kernel follow the FDT. As shown in Figures 5 (A-C), the normalized memory kernel and the RACF of the target molecules match each other, indicating compliance with FDT. From the RACF, we were able to obtain the Power Spectral Density (PSD) of the thermal noise as shown in Figures 5 (D-F), lets us observe the noise characteristics in the frequency domain. The PSD revealed that the noise is colored at high frequencies and white at low frequencies.

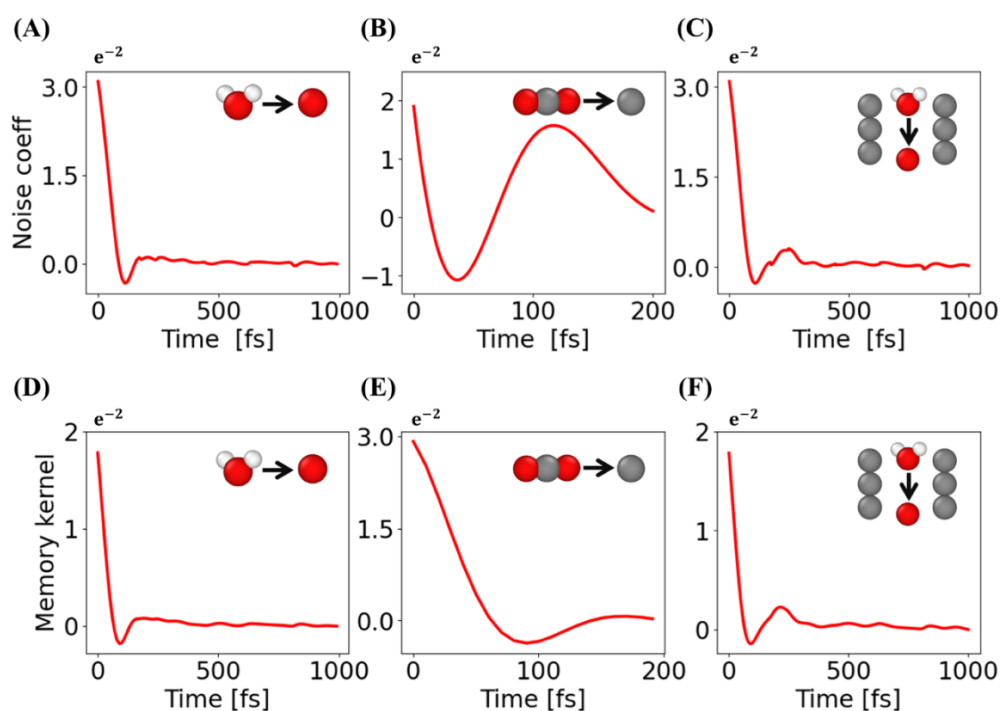


**Figure 4.** Learning results of the convolution filter and memory kernel from differentiable simulations. (A-C) Noise convolution filters for bulk water, bulk carbon dioxide, and confined water, respectively. (D-F) Isotropic memory kernels for bulk water, bulk carbon dioxide, and confined water.

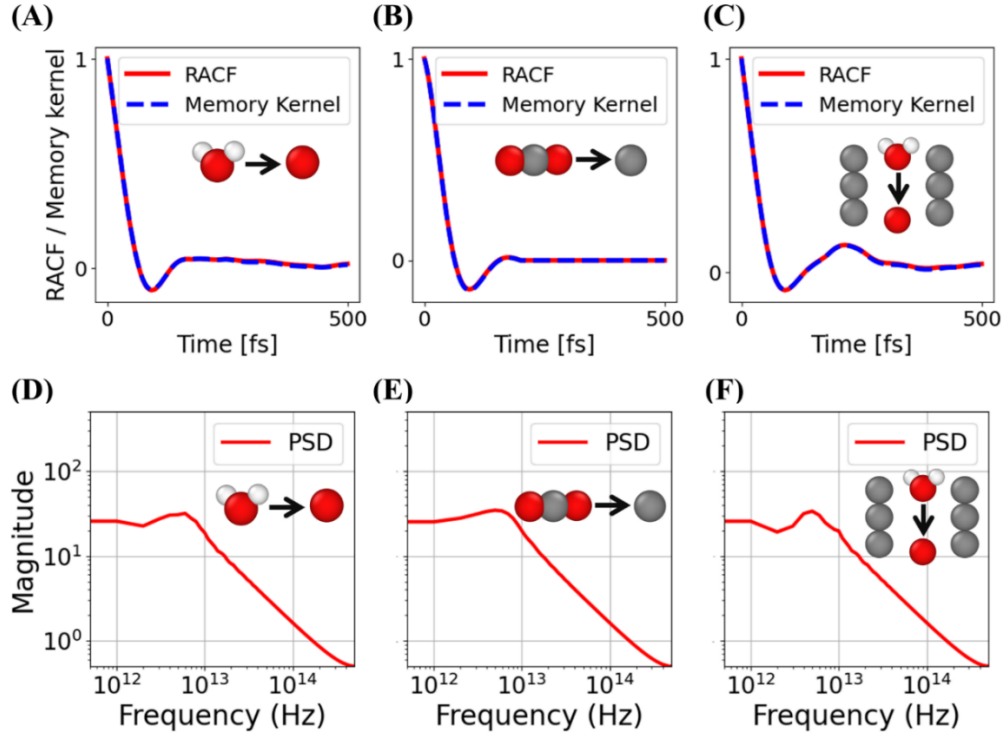


**Figure 5.** Validation of the FDT through comparison of the normalized memory kernel and the RACF. (A-C) Normalized memory kernel and RACF and (D-F) PSD of thermal noise for bulk water, bulk carbon dioxide, and confined water respectively.

#### 4. Conclusion

To conclude, we have developed a top-down method for parameterizing the non-Markovian GLE to construct dynamically accurate CG models. Our approach has been successfully applied to complex fluids such as SPC/E water and carbon dioxide, which exhibit intricate dynamic behaviour. By reformulating the GLE using a colored noise ansatz, we reframe the parameterization task as an inverse problem, learning the filter coefficients corresponding to the VACF of the original AA system. The resulting friction and stochastic forces inherently satisfy the FDT ensuring a physically consistent depiction of the system's dynamics. While top-down parameterization has traditionally posed significant challenges, we show that it becomes both achievable and efficient through the application of AD via the adjoint-state method. This method provides an efficient means to backpropagate gradients of a

scalar loss function on the VACF through the molecular dynamics simulation trajectory in a memory-efficient manner, enabling precise tuning of the filter coefficients to obtain accurate memory kernels and noise properties. This innovative approach opens new possibilities for parameterizing and developing different dynamically consistent CG models (like DPD and its variants<sup>22</sup>) with enhanced flexibility and simplicity, particularly in cases where a detailed bottom-up understanding of the system's time evolution is lacking or is computationally prohibitive such as that involving non-equilibrium systems<sup>46,47</sup>.

#### AUTHOR INFORMATION:

##### **Corresponding Author**

\*Email - [aluru@utexas.edu](mailto:aluru@utexas.edu)

##### **Notes**

The authors declare no competing interests.

#### ACKNOWLEDGEMENTS:

The work on deep learning was supported by the Center for Enhanced Nanofluidic Transport (CENT), an Energy Frontier Research Center funded by the U.S. Department of Energy, Office of Science, Basic Energy Sciences (Award No. DE-SC0019112). All other aspects of this work were supported by the National Science Foundation under Grant No 2137157. The authors acknowledge the Texas Advanced Computing Center (TACC) at The University of Texas at Austin for providing access to the Lonestar6 resource that has contributed to the research results reported within this paper. We also acknowledge the use of the Extreme Science and Engineering Discovery Environment (XSEDE) Stampede2 at the Texas Advanced Computing Centre through Allocation No. TG-CDA100010.

## References –

- (1) Noid, W. G. TopDown/Bottom up: Perspective: Coarse-Grained Models for Biomolecular Systems. *J. Chem. Phys.* **2013**, *139* (9), 090901. <https://doi.org/10.1063/1.4818908>.
- (2) Reith, D.; Pütz, M.; Müller-Plathe, F. Deriving Effective Mesoscale Potentials from Atomistic Simulations. *J. Comput. Chem.* **2003**, *24* (13), 1624–1636. <https://doi.org/10.1002/jcc.10307>.
- (3) Izvekov, S.; Voth, G. A. A Multiscale Coarse-Graining Method for Biomolecular Systems. *J. Phys. Chem. B* **2005**, *109* (7), 2469–2473. <https://doi.org/10.1021/jp044629q>.
- (4) Chaimovich, A.; Shell, M. S. Coarse-Graining Errors and Numerical Optimization Using a Relative Entropy Framework. *The Journal of Chemical Physics* **2011**, *134* (9), 094112. <https://doi.org/10.1063/1.3557038>.
- (5) Nadkarni, I.; Wu, H.; Aluru, N. R. Data-Driven Approach to Coarse-Graining Simple Liquids in Confinement. *J. Chem. Theory Comput.* **2023**. <https://doi.org/10.1021/acs.jctc.3c00633>.
- (6) Padding, J. T.; Briels, W. J. Systematic Coarse-Graining of the Dynamics of Entangled Polymer Melts: The Road from Chemistry to Rheology. *J. Phys.: Condens. Matter* **2011**, *23* (23), 233101. <https://doi.org/10.1088/0953-8984/23/23/233101>.
- (7) Tozzini, V. Coarse-Grained Models for Proteins. *Current Opinion in Structural Biology* **2005**, *15* (2), 144–150. <https://doi.org/10.1016/j.sbi.2005.02.005>.
- (8) Depa, P. K.; Maranas, J. K. Speed up of Dynamic Observables in Coarse-Grained Molecular-Dynamics Simulations of Unentangled Polymers. *The Journal of Chemical Physics* **2005**, *123* (9), 094901. <https://doi.org/10.1063/1.1997150>.
- (9) Depa, P.; Chen, C.; Maranas, J. K. Why Are Coarse-Grained Force Fields Too Fast? A Look at Dynamics of Four Coarse-Grained Polymers. *The Journal of Chemical Physics* **2011**, *134* (1), 014903. <https://doi.org/10.1063/1.3513365>.
- (10) Meinel, M. K.; Müller-Plathe, F. Loss of Molecular Roughness upon Coarse-Graining Predicts the Artificially Accelerated Mobility of Coarse-Grained Molecular Simulation Models. *J. Chem. Theory Comput.* **2020**, *16* (3), 1411–1419. <https://doi.org/10.1021/acs.jctc.9b00943>.
- (11) Mori, H. A Continued-Fraction Representation of the Time-Correlation Functions. *Progress of Theoretical Physics* **1965**, *34* (3), 399–416. <https://doi.org/10.1143/PTP.34.399>.
- (12) Zwanzig, R. Memory Effects in Irreversible Thermodynamics. *Phys. Rev.* **1961**, *124* (4), 983–992. <https://doi.org/10.1103/PhysRev.124.983>.
- (13) Hijón, C.; Español, P.; Vanden-Eijnden, E.; Delgado-Buscalioni, R. Mori–Zwanzig Formalism as a Practical Computational Tool. *Faraday Discuss.* **2009**, *144* (0), 301–322. <https://doi.org/10.1039/B902479B>.



- (14) Bereau, T.; Rudzinski, J. F. Accurate Structure-Based Coarse-Graining Leads to Consistent Barrier-Crossing Dynamics. *Phys. Rev. Lett.* **2018**, *121* (25), 256002. <https://doi.org/10.1103/PhysRevLett.121.256002>.
- (15) Song, J.; Hsu, D. D.; Shull, K. R.; Phelan, F. R. Jr.; Douglas, J. F.; Xia, W.; Keten, S. Energy Renormalization Method for the Coarse-Graining of Polymer Viscoelasticity. *Macromolecules* **2018**, *51* (10), 3818–3827. <https://doi.org/10.1021/acs.macromol.7b02560>.
- (16) Rudzinski, J. F. Recent Progress towards Chemically-Specific Coarse-Grained Simulation Models with Consistent Dynamical Properties. *Computation* **2019**, *7* (3), 42. <https://doi.org/10.3390/computation7030042>.
- (17) Klippenstein, V.; Tripathy, M.; Jung, G.; Schmid, F.; Van Der Vegt, N. F. A. Introducing Memory in Coarse-Grained Molecular Simulations. *J. Phys. Chem. B* **2021**, *125* (19), 4931–4954. <https://doi.org/10.1021/acs.jpccb.1c01120>.
- (18) Schilling, T. Coarse-Grained Modelling out of Equilibrium. *Physics Reports* **2022**, *972*, 1–45. <https://doi.org/10.1016/j.physrep.2022.04.006>.
- (19) Li, Z.; Bian, X.; Li, X.; Karniadakis, G. E. Incorporation of Memory Effects in Coarse-Grained Modeling via the Mori-Zwanzig Formalism. *The Journal of Chemical Physics* **2015**, *143* (24), 243128. <https://doi.org/10.1063/1.4935490>.
- (20) te Vrugt, M.; Wittkowski, R. Mori-Zwanzig Projection Operator Formalism for Far-from-Equilibrium Systems with Time-Dependent Hamiltonians. *Phys. Rev. E* **2019**, *99* (6), 062118. <https://doi.org/10.1103/PhysRevE.99.062118>.
- (21) Izvekov, S. Mori-Zwanzig Theory for Dissipative Forces in Coarse-Grained Dynamics in the Markov Limit. *Phys. Rev. E* **2017**, *95* (1), 013303. <https://doi.org/10.1103/PhysRevE.95.013303>.
- (22) Liu, M.; Yong, W.-A. Dissipative Particle Dynamics (DPD): An Overview and Recent Developments. *Arch. Comput. Methods Eng.* **2015**, *22* (4), 529–556. <https://doi.org/10.1007/s11831-014-9124-x>.
- (23) Yoshimoto, Y.; Kinefuchi, I.; Mima, T.; Fukushima, A.; Tokumasu, T.; Takagi, S. Bottom-up Construction of Interaction Models of Non-Markovian Dissipative Particle Dynamics. *Phys. Rev. E* **2013**, *88* (4), 043305. <https://doi.org/10.1103/PhysRevE.88.043305>.
- (24) Sanghi, T.; Aluru, N. R. Tarun-Thermal Noise in Confined Fluids. *The Journal of Chemical Physics* **2014**, *141* (17), 174707. <https://doi.org/10.1063/1.4900501>.
- (25) Klippenstein, V.; van der Vegt, N. F. A. Bottom-Up Informed and Iteratively Optimized Coarse-Grained Non-Markovian Water Models with Accurate Dynamics. *J. Chem. Theory Comput.* **2023**, *19* (4), 1099–1110. <https://doi.org/10.1021/acs.jctc.2c00871>.
- (26) Lesnicki, D.; Vuilleumier, R.; Carof, A.; Rotenberg, B. Molecular Hydrodynamics from Memory Kernels. *Phys. Rev. Lett.* **2016**, *116* (14), 147804. <https://doi.org/10.1103/PhysRevLett.116.147804>.

- (27) Lyu, L.; Lei, H. Construction of Coarse-Grained Molecular Dynamics with Many-Body Non-Markovian Memory. *Phys. Rev. Lett.* **2023**, *131* (17), 177301. <https://doi.org/10.1103/PhysRevLett.131.177301>.
- (28) Xie, P.; Qiu, Y.; E, W. Coarse-Graining Conformational Dynamics with Multi-Dimensional Generalized Langevin Equation: How, When, and Why. arXiv May 20, 2024. <http://arxiv.org/abs/2405.12356> (accessed 2024-07-12).
- (29) Izvekov, S. Microscopic Derivation of Particle-Based Coarse-Grained Dynamics. *The Journal of Chemical Physics* **2013**, *138* (13), 134106. <https://doi.org/10.1063/1.4795091>.
- (30) Kauzlaric, D.; Praprotnik, M.; Delgado-Buscalioni, R.; Kremer, K.; Ciccotti, G. Three Routes to the Friction Matrix and Their Application to the Coarse-Graining of Atomic Lattices. *Macromol. Theory Simul.* **2011**, *20* (6), 526–540. <https://doi.org/10.1002/mats.201100014>.
- (31) Baydin, A. G.; Pearlmutter, B. A.; Radul, A. A.; Siskind, J. M. Automatic Differentiation in Machine Learning: A Survey. arXiv February 5, 2018. <https://doi.org/10.48550/arXiv.1502.05767>.
- (32) Rumelhart, D. E.; Hinton, G. E.; Williams, R. J. Learning Representations by Back-Propagating Errors. *Nature* **1986**, *323* (6088), 533–536. <https://doi.org/10.1038/323533a0>.
- (33) Margossian, C. C. A Review of Automatic Differentiation and Its Efficient Implementation. *WIREs Data Min & Knowl* **2019**, *9* (4), e1305. <https://doi.org/10.1002/WIDM.1305>.
- (34) Schoenholz, S. S.; Cubuk, E. D. JAX, M.D.: A Framework for Differentiable Physics. arXiv December 3, 2020. <http://arxiv.org/abs/1912.04232> (accessed 2023-07-23).
- (35) Doerr, S.; Majewski, M.; Pérez, A.; Krämer, A.; Clementi, C.; Noe, F.; Giorgino, T.; De Fabritiis, G. TorchMD: A Deep Learning Framework for Molecular Simulations. *J. Chem. Theory Comput.* **2021**, *17* (4), 2355–2363. <https://doi.org/10.1021/acs.jctc.0c01343>.
- (36) Wang, X.; Li, J.; Yang, L.; Chen, F.; Wang, Y.; Chang, J.; Chen, J.; Feng, W.; Zhang, L.; Yu, K. DMFF: An Open-Source Automatic Differentiable Platform for Molecular Force Field Development and Molecular Dynamics Simulation. *J. Chem. Theory Comput.* **2023**, *19* (17), 5897–5909. <https://doi.org/10.1021/acs.jctc.2c01297>.
- (37) Thaler, S.; Zavadlav, J. Learning Neural Network Potentials from Experimental Data via Differentiable Trajectory Reweighting | Nature Communications. *Nature Communications* **2021**, *12* (1), 6884. <https://doi.org/10.1038/s41467-021-27241-4>.
- (38) Engel, M. C.; Smith, J. A.; Brenner, M. P. Optimal Control of Nonequilibrium Systems through Automatic Differentiation. arXiv December 31, 2021. <https://doi.org/10.48550/arXiv.2201.00098>.
- (39) Wang, W.; Axelrod, S.; Gómez-Bombarelli, R. Differentiable Molecular Simulations for Control and Learning. arXiv December 23, 2020. <https://doi.org/10.48550/arXiv.2003.00868>.

- (40) Shell, M. S. The Relative Entropy Is Fundamental to Multiscale and Inverse Thermodynamic Problems. *The Journal of Chemical Physics* **2008**, *129* (14), 144108. <https://doi.org/10.1063/1.2992060>.
- (41) Mashayak, S. Y.; Jochum, M. N.; Koschke, K.; Aluru, N. R.; Rühle, V.; Junghans, C. Relative Entropy and Optimization-Driven Coarse-Graining Methods in VOTCA. *PLOS ONE* **2015**, *10* (7), e0131754. <https://doi.org/10.1371/journal.pone.0131754>.
- (42) Chen, R. T. Q.; Rubanova, Y.; Bettencourt, J.; Duvenaud, D. K. Neural Ordinary Differential Equations. In *Advances in Neural Information Processing Systems*; Curran Associates, Inc., 2018; Vol. 31.
- (43) Lettermann, L.; Jurado, A.; Betz, T.; Wörgötter, F.; Herzog, S. Tutorial: A Beginner's Guide to Building a Representative Model of Dynamical Systems Using the Adjoint Method. *Commun Phys* **2024**, *7* (1), 1–14. <https://doi.org/10.1038/s42005-024-01606-9>.
- (44) Šípka, M.; Dietschreit, J. C. B.; Grajciar, L.; Gómez-Bombarelli, R. *Differentiable Simulations for Enhanced Sampling of Rare Events*. arXiv.org. <https://arxiv.org/abs/2301.03480v2> (accessed 2024-10-08).
- (45) Han, B.; Yu, K. Refining Potential Energy Surface through Dynamical Properties via Differentiable Molecular Simulation. arXiv June 27, 2024. <https://doi.org/10.48550/arXiv.2406.18269>.
- (46) Baiesi, M.; Maes, C.; Wynants, B. Fluctuations and Response of Nonequilibrium States. *Phys. Rev. Lett.* **2009**, *103* (1), 010602. <https://doi.org/10.1103/PhysRevLett.103.010602>.
- (47) Robertson, B. Equations of Motion in Nonequilibrium Statistical Mechanics. *Phys. Rev.* **1966**, *144* (1), 151–161. <https://doi.org/10.1103/PhysRev.144.151>.